

Structure of (*Z*)-(5*R*)-methyl-2-(4-phenylbenzylidene)cyclohexanone as chiral component of liquid-crystalline systems

A. I. Krivoshey,^a N. S. Pivnenko,^a S. V. Shishkina,^a A. V. Turov,^b L. A. Kutulya,^{a*} and O. V. Shishkin^a

^aScientific and Technological Corporation "Institute for Single Crystals", National Academy of Sciences of Ukraine, 60 prosp. Lenina, 61001 Kharkov, Ukraine.

Fax: +38 (057) 340 9343. E-mail: kutulya@isc.kharkov.com

^bT. G. Shevchenko Kiev National University, 4 ul. Vladimirska, 01033 Kiev, Ukraine

The spatial structure of (*Z*)-(5*R*)-methyl-2-(4-phenylbenzylidene)cyclohexanone prepared by photochemical isomerization of the *E*-isomer was studied by analyzing the magnitudes and temperature dependence of the proton spin-spin coupling constants obtained by ¹H NMR spectroscopy and the results of molecular modeling using semiempirical quantum chemical AM1 and PM3 methods and the density functional theory (DFT). Comparison of the results obtained for the *Z*- and *E*-isomers shows that in both cases the conformational equilibrium for both isomers is characterized by significant preference of the chair conformer having an equatorial methyl group, namely, $-\Delta H$ (chair *a* \rightleftharpoons chair *e*) = 1.98–2.12 and 1.36–1.54 kcal mole^{−1} for the *Z*- and *E*-isomers, respectively. Distinctions in the non-planarity of the enone fragment and cyclohexanone ring in the *Z*- and *E*-isomers under study following from the results of mathematical modeling were confirmed by the experimental values of the geminal spin-spin coupling constants of protons of the methylene groups in α, α' -positions with respect to the enone group. Quantum chemical calculations of the *Z*-isomer revealed the existence of intramolecular hydrogen bond between the carbonyl oxygen and the nearest aromatic proton in *ortho*-position of the benzene ring. Possible reasons for different helical twisting power of (*Z*)-(5*R*)-methyl-2-(4-phenylbenzylidene)cyclohexanone and the *E*- and *Z*-arylidene derivatives of 1*R*,4*R*-isomenthone in the mesophase are discussed based on the results of molecular structure studies for these compounds.

Key words: (*Z*)- and (*E*)-(5*R*)-methyl-2-(4-phenylbenzylidene)cyclohexanone, conformational state, ¹H NMR spectroscopy, quantum chemical calculations, intramolecular hydrogen bond.

Chiral α, β -unsaturated ketones with six-membered-ring preset *s-cis*-configuration of enone fragment and a *Z*- or *E*-configuration relative to the double bond are of considerable interest as components of liquid-crystalline (LC) systems with induced helical supramolecular ordering.^{1–4} Photoinduced effects in LC compositions, which accompany a reversible photochemical *E*–*Z*-isomerization typical of these compounds,^{5–9} strongly depend on the nature of both the nematic solvent and, especially, the chiral additive (CA), although the reasons for this dependence are unclear.

Photoactive CA include, in particular, 2-arylidene derivatives of (1*R*,4*R*)-isomenthone ((3*R*,6*R*)-6-isopropyl-3-methylcyclohexanone) **1***, which were studied in detail

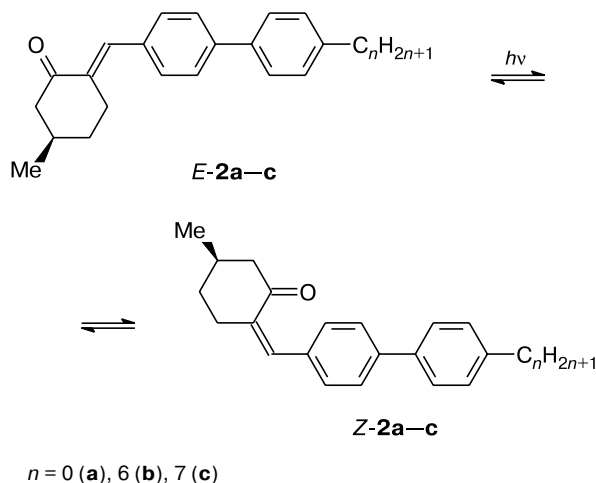
earlier.^{5,6,10,11} UV-Irradiation of *E*-isomers in both isotropic organic solvents^{5,10} and LC media^{5,11} causes a highly efficient *E*–*Z*-photoisomerization. A feature of this photochemical transformation consists in a higher quantum yield of the direct reaction compared to that of the reverse reaction. This predetermines a much higher proportion of the *Z*-isomer in the photostationary state.¹⁰ An important macroscopic manifestation of this photo-transformation in doped LC compositions is an increase in the pitch of the supramolecular helix (*P*), *i.e.*, its untwisting.^{5,11} A number of photochemically synthesized *Z*-isomers exhibited much less pronounced twisting properties compared to the *E*-isomers,^{5,6,11} which underlies the photoinduced untwisting of the cholesteric helix.

Recently,^{7,8} it was established that the *E*- and *Z*-isomers of monoarylidene derivatives of (3*R*)-methylcyclohexanone **2b,c** (Scheme 1) introduced into 4-(*n*-pentyl)-4'-cyanobiphenyl (5CB) nematic mesophase show a different ratio of the twisting powers (β), although both the

* In the text below the unsaturated ketones under study will be called "arylidene cyclohexanone derivatives" for convenience of comparing the characteristics of methylcyclohexanone and isomenthone derivatives.

ratio of the quantum yields of the direct and reverse photoisomerizations and the compositions of the photo-stationary mixture are almost the same as for the arylidene derivatives of isomenthone **1**.

Scheme 1



In this case the *E*- and *Z*-isomers are characterized by the opposite signs of β , i.e., they induce cholesteric helices with opposite directions of twisting in nematic liquid crystals. Unlike isomeric arylidene derivatives of isomenthone, in the series of (3*R*)-methylcyclohexanones **2** the isomer *Z*-**2b** obtained by preparative synthesis is characterized by a $|\beta|$ value that is 3.5–4 times higher than the corresponding value for the *E*-isomer (measured using different methods). This difference between the twisting properties of the isomers *E*-**2** and *Z*-**2** leads to photo-induced inversion of the cholesteric helix found for the LC system 5CB–CA *E*-**2c**.^{7,8} Recently, a qualitatively similar ratio of the twisting powers of the *E*- and *Z*-isomers was also observed⁹ for the arylidene derivatives of some other isomeric methyl-substituted cyclohexanones, which was not explained at that time.

A considerable weakening of the twisting properties of the *Z*-isomers compared to the *E*-isomers of the arylidene derivatives of compound **1** was associated with the less anisometric "twisted" molecular form of the former.^{4,5} At the same time, recent experimental data obtained for (3*R*)-methylcyclohexanone derivatives^{7,8} point to insufficiency of this interpretation. This gave an impetus to a more detailed investigation of the structure of the *Z*-mono-arylidene derivatives of (3*R*)-methylcyclohexanone.

The aim of this work was to study the structure of *Z*-arylidene cyclohexanone **2a** (*Z*-**2a**) obtained for the first time by ¹H NMR spectroscopy with implication of analysis of the temperature dependences of spectral parameters and the results of molecular modeling by the semiempirical quantum chemical methods AM1 and PM3 and by the

density functional theory (DFT). The first two computational methods have some drawbacks and limitations; nevertheless, they have been successively used earlier^{12–14} for the conformational analysis of related compounds and showed good agreement with experimental data. Simultaneously using all these methods in this work, we were interested in reconstructing a generalized picture of the spatial structure of the compounds under study and in making the structural data obtained more reliable rather than performing a comparative characterization of the results obtained by different modeling techniques. The results of our study of isomer *Z*-**2a** were compared with those obtained for *E*-**2a**,¹⁴ which is important for the understanding of the specific features of the behavior of these compounds in LC systems (see above). In order to assess with certainty structural differences between pairs of the *E*- and *Z*-isomers of the unsaturated ketones under study (in particular, the relative extent of non-planarity of the double bonds in the enone groups), we also compared the spectral characteristics of the long-wavelength π, π^* -band in the electronic absorption spectra and the stretching frequencies of the carbonyl group in the IR spectra. Based on the data on the spatial structure of the chiral unsaturated ketones *Z*-**2** in question, corresponding *E*-isomers, and their isomenthone analogs **1** we will discuss regularities of changes in the twisting properties of these pairs of isomers in the mesophase.

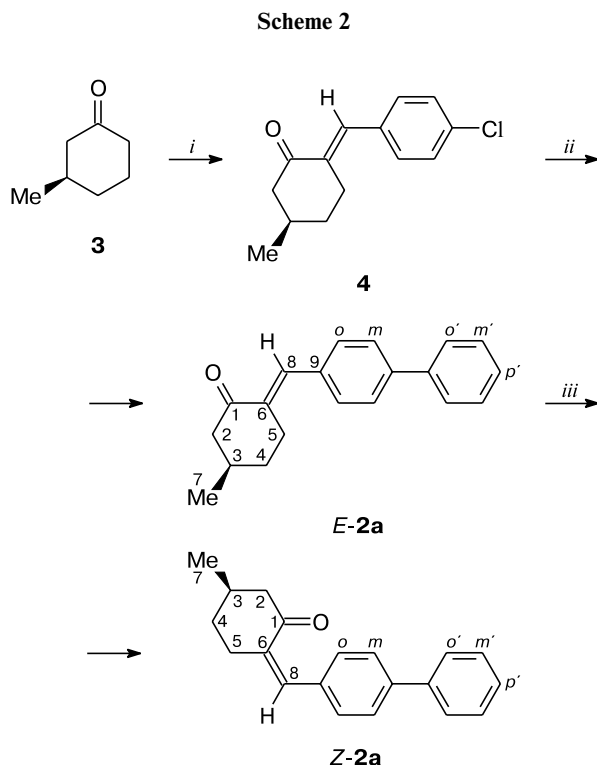
Results and Discussion

The compound in question, *Z*-**2a**, was obtained by photochemical transformation of corresponding *E*-isomer (*E*-**2a**, Scheme 2), which was synthesized starting from (3*R*)-methylcyclohexanone **3** in two stages (see Experimental).

A similar procedure was used¹⁵ for the synthesis of the compounds of the homologous series *E*-**2** with long terminal alkyl substituents C_nH_{2n+1} ($n = 7–11, 16$; e.g., *E*-**2b,c**). They are highly soluble in LC systems, being at the same time less suitable for detailed ¹H NMR studies of their structures compared to *E*-**2a**.

The reaction of 3-methylcyclohexanone (**3**) with 4-chlorobenzaldehyde in boiling aqueous alkali solution following a procedure similar to a known one¹⁶ results in enone **4** (yield 67%). This procedure is more preferable than the classical procedure for croton condensation of cyclohexanones by prolonged stirring a mixture of reagents in aqueous alkali at room temperature (yields 20–25%).¹⁷

Compound **4** interacts with phenylboronic acid under conditions of Suzuki cross-coupling catalyzed by *in situ* prepared nickel(0) complexes by analogy with a known procedure.¹⁸ Except for a few studies^{15,19,20} we found no information on the use of halo-substituted aromatic com-



Reagents and conditions: *i.* 4-Chlorobenzaldehyde, NaOH, H₂O, Δ, 24 h. *ii.* Phenylboronic acid, NiCl₂(PPh₃)₂/DPPF, BuLi, K₃PO₄·(2–3)H₂O, dioxane, Δ, 7–8 h. *iii.* hv, heptane.

pounds with enone fragment not involved in the reaction as electrophilic substrates in the Suzuki cross-coupling. In obtaining monoarylidene derivatives **2** the chloro derivative **4** was chosen as electrophilic substrate in this reaction because attempts to isolate the corresponding bromide in individual form failed (for detail, see Refs 15 and 20).

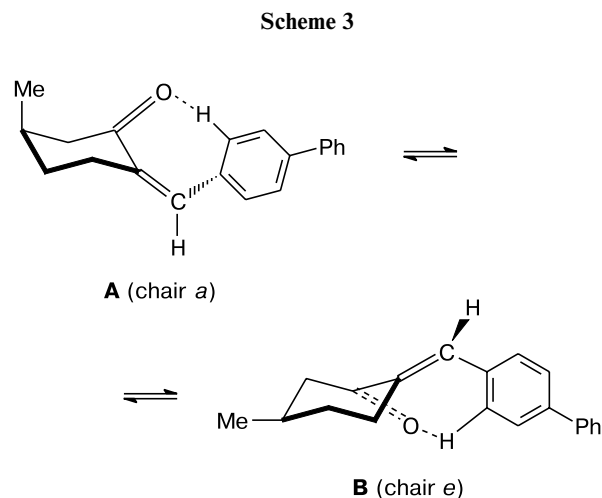
An attempt to carry out a cross-coupling reaction of 2-(4-chlorobenzylidene)-5-methylcyclohexanone (**4**) with phenylboronic acid under conditions of heterogeneous catalysis (palladium/carbon) in a dimethylacetamide–water mixture with potassium carbonate as base at 100 °C (see Ref. 21) failed owing to instability of product **2** and the starting compound **4** in a strongly basic medium at high temperature.

The configuration of isomer *Z*-**2a** was unambiguously confirmed by the diamagnetic shift of the signal of the arylidene proton ($\delta_{\text{CH}} = 6.43$) (Table 1) relative to the corresponding signal of the *E*-form ($\delta_{\text{CH}} = 7.53$), which is accepted^{22,23} as criterion for related structures, and by the lack of the NOE between protons in the cyclohexanone and aryl moieties. For the *E*-isomer, the NOE occurs between the aromatic *ortho*-protons and H(5) cyclohexanone protons separated by 2.32–2.47 (AM1 calculations) or 2.04–2.34 Å (DFT).

Table 1. Chemical shifts (δ) and spin-spin coupling constants ($J_{\text{H,H}}$) in ¹H NMR spectra of the *Z*- and *E*-isomers of compound **2a** (CDCl₃, 400 MHz, 293 K)

Proton	δ		Protons	$J_{\text{H,H}}/\text{Hz}$	
	<i>Z</i> - 2a	<i>E</i> - 2a		<i>Z</i> - 2a	<i>E</i> - 2a
H _{ax} (2)	2.272	2.113	H _{ax} (2), H _{eq} (2)	–14.0	–17.1
H _{eq} (2)	2.633	2.688	H _{ax} (2), H _{ax} (3)	11.5	11.4
H _{ax} (3)	2.116	2.076	H _{eq} (2), H _{ax} (3)	4.1	4.7
H _{ax} (4)	1.564	1.382	H _{eq} (2), H _{eq} (4)	1.9	2.4
H _{eq} (4)	2.011	1.935	H _{ax} (3), H _{ax} (4)	10.9	11.0
H _{ax} (5)	2.579	2.704	H _{ax} (3), H _{eq} (4)	3.7	3.1
H _{eq} (5)	2.705	3.109	H _{ax} (4), H _{eq} (4)	–12.9	–13.0
C(7)H ₃	1.078	1.063	H _{ax} (4), H _{ax} (5)	11.9	11.9
H(8)	6.430	7.533	H _{ax} (4), H _{eq} (5)	4.2	4.8
H _o	7.419	7.497	H _{eq} (4), H _{ax} (5)	4.2	5.4
H _m	7.513	7.625	H _{eq} (4), H _{eq} (5)	3.4	3.6
H _{o'}	7.579	7.613	H _{ax} (5), H _{eq} (5)	–14.3	–16.4
H _{m'}	7.426	7.455	H _{ax} (5), H(8)	2.0	2.6
H _{p'}	7.332	7.369	H _{eq} (5), H(8)	0.5	1.7
			H(3), C(7)H ₃	6.5	6.2

Conformational state of cyclohexanone fragment. Most probably, isomer *Z*-**2a** exists in solutions as an equilibrium mixture of chair conformers with axial and equatorial orientation of methyl group, similarly to *E*-**2a**¹⁴ (Scheme 3).



It should be noted that in monoalkyl-substituted cyclohexanes the substituent has only equatorial orientation.²⁴ However, isomeric alkylcyclohexanones, especially those containing an extra unsaturated substituent, can exist as equilibrium mixtures of the chair-*e* (equatorial), chair-*a* (axial), and even twist-conformers (see, *e.g.*, Refs 12, 13, 25–27). Some compounds of this type exist as mixtures with a very high proportion of the conformation with axial orientation of the methyl substituent.^{12,28}

A number of 2-arylidene derivatives of (3*R*,6*S*)-6-isopropyl-3-methylcyclohexanone have different conformational structures in solutions¹³ and in crystals.²⁹ We failed to find information on the molecular conformations of chiral *Z*-isomers of α,β -unsaturated ketones except for the data reported in Ref. 12. Because the twisting properties of this type of chiral compounds depend on the orientation of alkyl substituent in the cyclohexanone ring that fixes the *s-cis*-enone group,⁹ it was important to study the conformational equilibrium (see Scheme 3) for the isomer **Z-2a**. Information on the effect of the *Z*- or *E*-arylidene substituent in the cyclohexanone ring on the conformational equilibrium is also of fundamental interest.

Similarly to isomer *E-2a*,¹⁴ the AM1 and PM3 calculations of isomer **Z-2a** revealed very small proportions of twist-conformers (Table 2). According to DFT calculations, the twist-conformers have much higher energies and can therefore be left out of consideration.

The conformational equilibrium mentioned above (see Scheme 3) was studied by analogy with that reported earlier¹⁴ based on the analysis of the magnitudes and temperature dependences of vicinal spin-spin coupling constants (³*J*) and on the results of molecular modeling using the AM1, PM3, and DFT methods. According to calculations (see Table 2), the **Z-2a** isomer exists mainly in conformation **B** (83.5% according to AM1 and PM3 calculations) similarly to *E-2a*.¹⁴ This is the total mole fraction of the two rotamers obtained from the results of modeling for each type of conformers. The rotamers differ in the direction of rotation of the benzene ring relative

to the double bond (the sign of the angle φ_{Ph}) and have different energies. The calculated energies of conformer **A** exceed those of the equatorial conformers (taking into account correspondence between the rotamers) by 1.27–1.29 (AM1) and 1.04–1.05 kcal mol^{−1} (PM3) (see Table 2). The results of the semiempirical and DFT calculations are by and large in agreement, although the last-mentioned method does not predict the existence of two types of rotamers of the *Z*-isomer, but predicts a somewhat greater energy preferableness (1.64 kcal mol^{−1}) and, hence, higher proportion of the conformer **B** (94.2%) (Table 3).

Similar proportions of the alternative conformers were also predicted by the semiempirical methods for isomer *E-2a*.¹⁴ DFT calculations in this case predict a somewhat higher energy preferableness of the equatorial form (2.04–2.18 kcal mol^{−1}; see Table 3) and reflect the existence of pairs of rotamers for each type of conformers.

Our investigation of the conformational equilibrium of isomers **Z-2a** and *E-2a* was based on the results of ¹H NMR study. The experimental (*a*) and calculated (*b*) multiplets of protons in the cyclohexanone ring of compound **Z-2a** in CDCl₃ at 20 °C are shown in Fig. 1. Table 1 lists the proton chemical shifts and spin-spin coupling constants for **Z-2a** and *E-2a*. At all temperatures, the multiplet of H_{ax}(2) proton is most pronounced for both compounds under study.

The conformer ratio, $m_{\text{eq}}/m_{\text{ax}}$ (m_{eq} and m_{ax} are the mole fractions of the conformers **B** and **A** correspondingly) was determined based on the analysis of conformationally sensitive vicinal constant ³*J*_{2ax,3} from the multi-

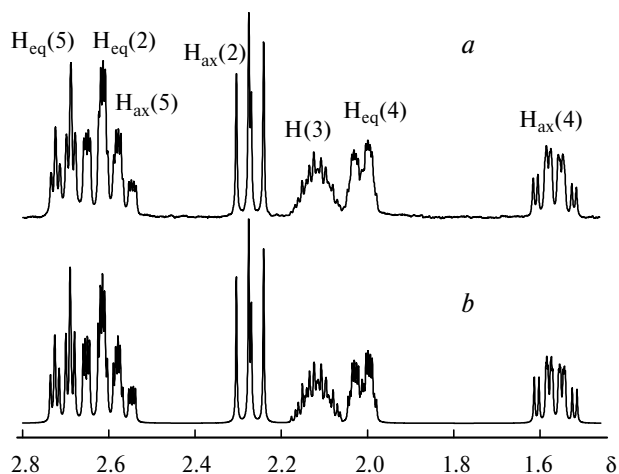
Table 2. Energies (*E*) and selected geometric parameters of alternative conformers of isomer **Z-2a** obtained from AM1 and PM3 calculations

Conformer	<i>E</i> /kcal mol ^{−1}	Proportion (%)	φ_{Ph}	φ_{enon}	θ_1	θ_2	$d_{\text{C=O...H-Ar}}$ /Å
deg							
AM1							
B ₁ , chair <i>e</i> -1	0.0	57.57	−45.4	57.8	108	122	2.20
B ₂ , chair <i>e</i> -2	0.47	25.96	24.9	53.9	71	110	2.54
A ₁ , chair <i>a</i> -1	1.27	6.69	43.6	−58.2	107	124	2.19
A ₂ , chair <i>a</i> -2	1.76	2.92	−25.0	−54.5	71	110	2.55
T ₁ , twist-1	1.48	4.69	43.5	−59.8	—	—	2.18
T ₂ , twist-2	1.93	2.19	−20.0	−57.6	—	—	2.48
PM3							
B ₁ , chair <i>e</i> -1	0.0	51.38	44.1	58.7	60	93	3.08
B ₂ , chair <i>e</i> -2	0.28	31.97	−63.9	58.9	105	104	2.64
A ₁ , chair <i>a</i> -1	1.04	8.82	−43.9	−58.9	60	93	3.07
A ₂ , chair <i>a</i> -2	1.33	5.39	63.2	−59.3	105	105	2.63
T ₁ , twist-1	2.39	0.89	65.0	−60.5	—	—	2.65
T ₂ , twist-2	2.07	1.54	−42.0	−60.4	—	—	3.04

Note. Here and in Table 3 φ_{enon} is the torsion angle O—C(1)—C(6)—C(8), φ_{Ph} is the torsion angle C(6)—C(8)—C(9)—C_O, θ_1 is the angle C(1)=O...H_{Ar}, θ_2 is the angle O...H_{Ar}—C_{Ar}, and $d_{\text{C=O...H-Ar}}$ is the distance from the carbonyl O atom to the nearest aromatic proton.

Table 3. Energies (*E*) and selected geometric parameters of alternative conformers of isomers *Z*-**2a** and *E*-**2a** (modeling by DFT and MP2 methods)

Conformer	$E/\text{kcal mol}^{-1}$		Proportion (%)		φ_{Ph}	φ_{enon}	φ_{CH_3}	θ_1	θ_2	$d_{\text{C}=\text{O}\cdots\text{H}-\text{Ar}}$ /Å
	DFT	MP2	DFT	MP2						
deg										
<i>Z</i> - 2a										
B , chair <i>e</i>	0.00	0.00	94.16	79.51	−25.4	42.1	175	114	136	2.07
A , chair <i>a</i>	1.64	0.80	5.84	20.49	27.1	−43.9	74.3	114	136	2.07
<i>E</i> - 2a										
B ₁ , chair <i>e</i> -1	0.00	0.00	90.85	77.18	21.1	9.4	173	—	—	—
B ₂ , chair <i>e</i> -2	2.04	1.80	2.86	3.65	−35.9	15.9	173	—	—	—
A ₁ , chair <i>a</i> -1	1.59	0.84	6.14	18.59	−19.2	−9.5	74.7	—	—	—
A ₂ , chair <i>a</i> -2	3.77	2.88	0.16	0.59	35.6	−15.5	75.7	—	—	—

**Fig. 1.** Experimental (*a*) and calculated (*b*) multiplets of cyclohexanone ring protons in ¹H NMR spectra of compound *Z*-**2a** (400 MHz, CDCl₃).

plet of H_{ax}(2) proton (see above) with allowance for the weight-averaged nature of the observed quantity

$$^3J_{2ax,3} = m_{eq}J_{eq} + m_{ax}J_{ax},$$

where *J*_{eq} and *J*_{ax} are the spin-spin coupling constants of conformers **B** and **A**, respectively. The *J*_{eq} and *J*_{ax} values

were calculated based on the optimized geometries of the alternative conformers in the framework of the computational methods employed (similarly to our previous study¹⁴) using the known equation.³⁰ It should be noted that the use of the geometry of the cyclohexanone fragment calculated by the AM1 and PM3 methods and by the DFT method gives almost the same calculated values of the spin-spin coupling constants of the conformers (*J*_{eq} and *J*_{ax}) and, correspondingly, the ratios of their concentrations. This can indicate that all the three methods correctly describe the geometry of the cyclohexane ring in the compounds under study.

The calculated constants of conformational equilibrium, *K* = *m*_{eq}/*m*_{ax}, the corresponding conformational energies (Δ*G* = -*RT*ln*K*) at different temperatures, and the changes in the enthalpy (Δ*H*) and entropy (Δ*S*) of the conformational equilibrium are listed in Table 4. The parameters Δ*H* and Δ*S* were determined from the dependence of -Δ*G*/*T* on 1/*T* (correlation coefficients of linear approximation vary in the range 0.995–0.999). It should be noted that the constants and thermodynamic characteristics of the conformational equilibrium obtained from not only ³*J*_{2ax,3}, but also other experimental conformationally sensitive spin-spin coupling constants (³*J*_{3,4ax}, ³*J*_{4ax,5ax}) determined by simulating the corresponding

Table 4. Concentrations of equatorial conformer (*m*_{eq}, mole fractions), -Δ*G* (kcal mol⁻¹) values for the conformational equilibrium (see Scheme 3) of isomers *Z*-**2a** and *E*-**2a** at different temperatures according to ¹H NMR spectroscopy data (³*J*_{2ax,3}), and calculated Δ*H* and Δ*S* values

Method	$m_{\text{eq}}/-\Delta G$ at T/K						$-\Delta H$ /kcal mol ⁻¹	ΔS /cal K ⁻¹ mol ⁻¹
	238	248	253	273	293	323		
<i>Z</i> -Isomer								
AM1	0.952/1.41	0.943/1.38	—	—	0.897/1.24	—	2.07±0.06	2.8±0.2
PM3	0.949/1.38	0.940/1.36	—	—	0.894/1.24	—	1.98±0.01	2.5±0.1
DFT	0.953/1.42	0.944/1.39	—	—	0.898/1.27	—	2.12±0.04	2.9±0.2
<i>E</i> -Isomer								
AM1	0.926/1.20	—	0.917/1.21	0.899/1.19	0.881/1.17	0.854/1.13	1.39±0.2	0.8±0.1
PM3	0.922/1.17	—	0.913/1.18	0.894/1.16	0.876/1.14	0.849/1.11	1.36±0.2	0.8±0.5
DFT	0.936/1.27	—	0.927/1.28	0.909/1.25	0.890/1.22	0.863/1.18	1.54±0.2	1.1±0.5

multiplets characterized by larger broadening of their components with a decrease in temperature, are quite similar to those listed in Table 4 and found from the most reliably determined $^3J_{2ax,3}$ values.

The experimental ΔH values obtained for the conformational equilibrium of the isomeric ketones under study are in reasonable agreement with the calculated ΔE values (heat of formation difference, ΔH , between the conformers). The entropy contribution to the conformational energy of the compounds studied is small; this is also assumed to be typical of, in particular, monosubstituted cyclohexanes containing a spherical substituent (e.g., a methyl group).²⁴

From Table 4 it follows that compound *Z*-**2a** has a higher conformational energy ΔG at all measurement temperatures and is characterized by a more negative change in the enthalpy, ΔH , of conformational conversion (see Scheme 3) compared to isomer *E*-**2a**. Although the changes in entropy of the conformational equilibrium in question are small, the ΔS for these isomers differ with certainty; the entropy factor undoubtedly plays a more important role for the *Z*-isomer.

The experimental ΔH values for *E*-**2a** (see Table 4) almost coincide with the ΔH value for 3-methylcyclohexanone (-1.28 — -1.40 kcal mol⁻¹),²⁷ determined in the same solvent (CDCl₃) from the temperature dependence of the chemical shifts in the ¹³C NMR spectra. It follows that introduction of the second sp² carbon atom into the 3-methylcyclohexanone molecule to give a cinnamoyl fragment with *E*-configuration has no effect on the energy characteristics of the axial-equatorial conformational equilibrium. At the same time the characteristics of this equilibrium for *Z*-**2a** are significantly different from those of the *E*-isomer, namely, the differences between the corresponding ΔH values much exceed the experimental error. This is undoubtedly related to the structural features of isomers.

Geminal spin-spin coupling constants and the structure of the cyclohexanone and enone fragments. The geminal constants $^2J_{2ax,2eq}$ and $^2J_{5ax,5eq}$ of compound *Z*-**2a** (-14.0 and -14.4 Hz, respectively, see Table 1) are strongly different from those found for isomer *E*-**2a** (-17.2 and -16.4 Hz, respectively).¹⁴ The change in the 2J constants on going from the *E*- to the *Z*-isomer indicates different orientations of the π -bonds of the enone group relative to the α, α' -methylene units in the cyclohexanone rings in these molecules. The $^2J_{H,H}$ constant of the methylene group in α -position relative to the C=O or C=C bonds is determined as follows³¹:

$$^2J_{H,H} = -12.6 - 6.0\cos^2\varphi_{C=O}, \quad (1)$$

$$^2J_{H,H} = -11.6 - 6.3\cos^2\varphi_{C=C}, \quad (2)$$

where $\varphi_{C=O}$ and $\varphi_{C=C}$ are the torsion angles between the C=O or C=C groups and the bonds of the α -methylene

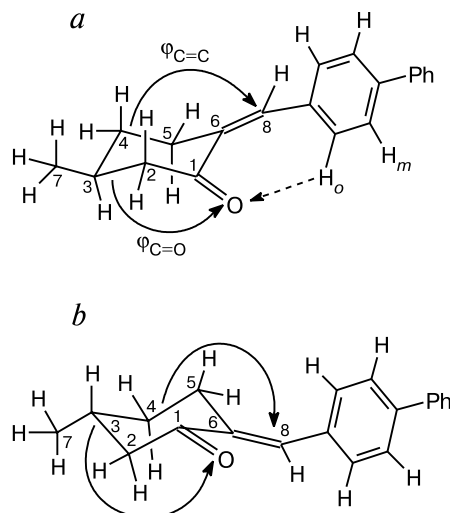


Fig. 2. Definition of torsion angles between the carbonyl ($\varphi_{C=O} = \varphi_{C(3)-C(2)-C(1)-O}$) or vinylenic ($\varphi_{C=C} = \varphi_{C(4)-C(5)-C(6)-C(8)}$) groups and the bonds in the α -methylene fragments with corresponding neighboring units of $>C(3)HCH_3$ or $>C(4)H_2$ rings in *Z*- (a) and *E*-isomers (b).

fragments with the corresponding neighboring alkyl fragments (definition of the angles φ for the *Z*- and *E*-isomers under study is shown in Fig. 2). From Eqs (1) and (2) it follows that the conformations with $\varphi_{C=O}$ or $\varphi_{C=C} = 0^\circ$ and with $\varphi_{C=O}$ or $\varphi_{C=C} = 180^\circ$ correspond to structures with maximum values of the constant 2J . The angles $\varphi_{C=O}$ and $\varphi_{C=C}$ (for notations, see Fig. 2) determined using the molecular geometries obtained by different methods and the geminal spin-spin coupling constants calculated from Eqs (1) and (2) are listed in Table 5. For comparison, we also present here the corresponding parameters of the *E*-isomer. The results obtained by all computational methods are in reasonable agreement and show, in accordance with the experimental data, higher values of the 2J constants for the *E*-isomers. The torsion angles $\varphi_{C=O}$ and $\varphi_{C=C}$ for the *Z*-isomer are smaller than for the *E*-isomer, which indicates an increase in the deviation of methylene groups from the plane of the double bonds. This favors a decrease in the overlap of the π -orbitals of the multiple bonds and the 1s-orbitals of the C—H bonds of methylene groups and, correspondingly, a decrease in the geminal spin-spin coupling constants.

Different geometries of the *Z*- and *E*-isomers also manifest themselves in the degree of non-planarity of the enone fragment. According to the results of modeling by all three computational methods, it is much more pronounced for isomer *Z*-**2** rather than *E*-**2** (see Ref. 14 and Tables 2 and 3). This difference in the geometry of the isomers can be experimentally substantiated by the UV and IR spectroscopy data. The long-wavelength π, π^* -band in the UV spectrum of *Z*-**2a** (298 nm) experiences a blue shift relative to the corresponding band of *E*-**2a** (312 nm).

Table 5. Selected torsion angles (φ_i /deg) (see Fig. 2) and calculated geminal spin-spin coupling constants of protons at the C(2) and C(5) atoms ($^2J_{\text{calc}}$ /Hz) in isomers **Z-2a** and **E-2a** (according to AM1, PM3, and DFT calculations)

Method	φ_{Ph}	$\text{H}_{\text{eq}}(2), \text{H}_{\text{ax}}(2)$		$\text{H}_{\text{ax}}(5), \text{H}_{\text{eq}}(5)$	
		$\varphi_{\text{C=O}}$	$-^2J_{\text{calc}}$	$\varphi_{\text{C=C}}$	$-^2J_{\text{calc}}$
<i>Z-2a</i>					
AM1	-45.4,	125.4,	14.6,	124.1,	13.6,
	24.9	125.7	14.6	127.7	14.0
PM3	44.1,	123.9,	14.5,	123.9,	13.6,
	-63.9	124.1	14.5	123.5	13.5
DFT	-26.1	138.9	16.0	129.5	14.1
			(14.4)		(14.0)
<i>E-2a</i>					
AM1	46.4,	142.8,	16.4,	142.3,	15.5,
	-57.2	140.7	16.2	139.0	15.2
PM3	-63.7,	133.9,	15.5,	132.6,	14.5,
	57.3	134.5	15.6	134.6	14.7
DFT	22.6,	157.5,	17.7,	155.9,	16.8,
	-37.0	152.8	17.3	148.5	16.2
			(17.2)		(16.4)

Note. Figures in parentheses denote the $-^2J_{\text{exp}}$ values.

The stretching frequency of the carbonyl group ($\nu(\text{C=O})$) in **Z-2a** (1695.2 cm^{-1}) is much higher than that of **E-2a** (1680.6 cm^{-1}). These differences between the spectral characteristics indicate a weaker electronic interaction in the enone moiety and, therefore, a more non-planar structure of this fragment in the *Z*-isomer. This structural distinction can be an important reason for different twisting powers of these compounds^{7,8} with allowance for the concept^{4,32} of the role of helical chirality of the additive molecules in the efficiency of inducing helical supramolecular ordering in the mesophase.

Structure of cinnamoyl fragment and hydrogen bond $\text{C}_{\text{arom}}-\text{H}\cdots\text{O}=\text{C}$. An important feature of compound **Z-2a** is the energy difference between rotamers of the benzylidene fragment, which follow from the results of modeling of pairs of corresponding conformers (see Tables 2 and 3). Semiempirical methods (AM1 and PM3) and the DFT method describe these distinctions in different manner.

According to AM1 calculations, rotamers with a shortened contact between the carbonyl oxygen and the nearest hydrogen atom in *ortho*-position of the benzene ring (chair *e*-1, chair *a*-1; see Table 2) are more preferable for each pair of conformers of cyclohexanone ring. The distance between these atoms and the magnitudes of the angles θ_1 ($\text{C}=\text{O}\cdots\text{H}_{\text{Ar}}$) and θ_2 ($\text{O}\cdots\text{H}_{\text{Ar}}-\text{C}_{\text{Ar}}$) in these conformers suggest the formation of intramolecular hydrogen bond $\text{C}-\text{H}\cdots\text{O}$ in this case. The existence of similar interactions in solutions was a debated topic for long,³³ the undirectedness of the interactions (*i.e.*, weak dependence of the $\text{C}-\text{H}\cdots\text{O}$ bond energy on the angle between

the $\text{O}\cdots\text{H}$ and $\text{H}-\text{C}$ bonds) being a major counter-argument. Nevertheless, the results of analysis of X-ray diffraction data almost undoubtedly indicate the possibility for hydrogen bonds $\text{C}-\text{H}\cdots\text{O}$ to exist in crystals.^{33,34} By and large at present it is accepted that hydrogen bonds $\text{C}-\text{H}\cdots\text{O}$ are characterized by $\text{O}\cdots\text{H}$ (here, $d_{\text{C}=\text{O}\cdots\text{H}-\text{Ar}}$) distances of at most 2.7 Å at an angle, θ_2 , between the $\text{O}\cdots\text{H}$ and $\text{H}-\text{C}$ bonds of at least 90° .³³ The calculated geometric characteristics of the shortened contacts in the chair *e*-1 and chair *a*-1 conformers of compound **Z-2a** (2.2–2.6 Å; see Table 2) lie in the intervals accepted for lengths of the hydrogen bonds $\text{C}-\text{H}\cdots\text{O}$.

Scanning the potential energy surface over the torsion angle φ_{Ph} by the AM1 method showed that the minimum distance between the carbonyl oxygen and the closest aromatic proton corresponds to a global energy minimum for the molecule. Additionally, the minimum $d_{\text{C}=\text{O}\cdots\text{H}-\text{Ar}}$ value logically corresponds to the maximum values of the $\text{C}_{\text{Ar}}-\text{H}$ bond length and the absolute values of the atomic charges of the carbonyl oxygen and aromatic proton. PM3 calculations gives some preference (by ~ 0.3 kcal mol^{-1}) to those rotamers of the arylidene fragment in which the aromatic *ortho*-proton is more distant from the carbonyl group (3.1 Å; see Table 2) and the formation of hydrogen bond is almost impossible. Therefore, in order to more reliably establish the nature of the shortened contact $\text{C}=\text{O}\cdots\text{H}-\text{Ar}$ in molecules **Z-2a**, we used the DFT B3LYP/cc-pVDZ method. Geometry optimization of the conformers with the shortened contact $\text{C}=\text{O}\cdots\text{H}-\text{Ar}$ using the geometric parameters obtained from AM1 and PM3 calculations as the starting approximation led to structures with a shortened contact (chair *e* and chair *a*, 2.07–2.08 Å, $\theta_1 = 114^\circ$ and $\theta_2 = 136^\circ$; see Table 3). The geometric parameters of the hydrogen bonds for the conformers with equatorial and axial methyl group are almost the same. It is important that calculations with the geometric parameters of the alternative rotamers of the arylidene fragment taken as the initial approximation also lead to conformers with hydrogen bonds $\text{C}-\text{H}\cdots\text{O}$, which are structurally similar to the chair *e* and chair *a* conformers. This can indicate realization of the one and only rotamer of the arylidene fragment. At the same time equivalence of the aromatic *o*- and *o'*-protons in the ^1H NMR spectrum of compound **Z-2a** (see Table 1) points to a rather high (on the time scale of NMR experiments) rotation rate of the benzene ring relative to the double bond of the enone fragment.

Positive harmonic vibrational frequencies calculated using the GAUSSIAN 98 program package³⁵ (by analogy with those reported earlier³⁶) for the chair *e* and chair *a* conformers (22.2 and 23.1 cm^{-1} , respectively) indicate that they correspond to energy minima. Topological analysis of the electron density distribution according to Bader³⁷ in the chair *e* conformer showed the presence of an axis connecting the oxygen atom and the nearest aromatic

o-proton, a (3, -1) critical point (electron density 0.023 au, Laplacian of electron density is 0.072 au), which corresponds to an attractive interaction between these atoms.

Thus, the results of AM1 and DFT B3LYP/cc-pVDZ quantum chemical calculations including the determination of harmonic vibrational frequencies and topological analysis of the electron density distribution indicate the occurrence of a specific nonvalence interaction, namely, intramolecular hydrogen bond C—H...O, in the molecules of isomer *Z*-**2a**. Although the energy of this hydrogen bond is low, it most likely stabilizes the arylidene fragment of the *Z*-isomer, which has a more non-planar enone group than the *E*-isomer, and, correspondingly, a higher degree of helical chirality.

Structural differences between the *Z*- and *E*-isomers of arylidene derivatives **1** and **2** underlie a qualitative model proposed^{20,38} for the description of the regularities of helical supramolecular ordering induced by the CAs **1** and **2** upon introduction into the nematic mesophase 5CB. The model is based on the assumption that the efficiency of helical twisting in the nematic mesophase doped with chiral compounds is determined by the balance between the attractive forces and stereospecific repulsion between the nematic and CA molecules. In the case of LC systems containing arylidene derivatives **1** and **2** the attractive factors first of all include the dispersion interactions between the benzene rings of the arylidene fragment of CA and the biphenyl group in the 5CB molecule. The attainment of a maximum energy gain for this interaction requires parallel alignment of these molecular fragments relative to each other and the presence of a certain optimum number of benzene rings in the CA molecules.

Intermolecular repulsion in a model system containing a CA molecule and two nematic molecules (arranged "above" and "below" relative to the additives) determines the direction of twisting (sign of β) and the angle between the long axes of 5CB molecules responsible for the $|\beta|$ value. We considered several types of molecular repulsion in the systems under study, having both steric and dipole-dipole nature. The main types were as follows: steric repulsion between the biphenyl fragment of 5CB molecule and the methyl group at the chiral center of CA (it is particularly important for CA **1** having an axially oriented methyl group^{12,13}) and electrostatic repulsion between the likely charged atoms of polar groups of the nematic (nitrile group) and additive (carbonyl and polarized arylidene double bond) molecules. Polarization of these groups of the components of liquid crystals and related effects of intermolecular repulsion in the mesophase depend on the molecular conformation including the stereospecific twisting of the enone fragment in a regular fashion.

As substantiated earlier,^{20,38} the former type of molecular repulsion in mesophase plays a decisive role for the LC system containing isomer *E*-**1a**, which exists in

solution and in the crystal in the conformation with axial methyl group,^{12,39} predetermining the formation of a left cholesteric helix* at a rather high twisting power ($\beta = -36.9 \pm 1.3 \mu\text{m}^{-1}$ (mole fraction)⁻¹).⁶ In the system 5CB—*Z*-**1a**, the equilibrium between the axial and equatorial CA conformers ($\sim 80 : 20$)¹² is responsible for the compensation effects; as a result, the *Z*-isomer is characterized by $\beta = -1.1 \pm 0.2 \mu\text{m}^{-1}$ (mole fraction)⁻¹,⁶ which is lower than for the *E*-isomer.

The conformational state of both *E*- and *Z*-isomers of arylidene derivatives of (3*R*)-methylcyclohexanone **2** is significantly different from that of their analogs **1**. In the framework of the model used in both cases it is assumed^{20,38} that repulsion between the biphenyl fragments of the 5CB molecules and the methyl group of the predominant equatorial CA conformer is insignificant owing to a long distance between these fragments in the interacting molecules. However, for the system 5CB—*E*-**2a** the dipole-dipole interactions between the negative ends of the nitrile (nematic) and carbonyl (CA) dipoles become significant. This leads to a counterclockwise rotation of the two 5CB molecules relative to each other (left supramolecular helix similar to the case of *E*-**1a**). Due to the lack of orientation effect of the axial methyl group the angle of rotation was estimated qualitatively as being much smaller than in the LC system containing the CA *E*-**1a**. These conclusions following from the qualitative model of twisting are in agreement with the experimental data (for *E*-**2a** $\beta = -7.7 \pm 0.5 \mu\text{m}^{-1}$ (mole fraction)⁻¹).²⁰

A particularly remarkable distinction between the properties of arylidene derivatives of compounds **1** and **2** is the positive sign and high twisting power of isomer *Z*-**2a** ($\beta = +37.4 \pm 1.9 \mu\text{m}^{-1}$ (mole fraction)⁻¹).³⁸ This cannot be interpreted unambiguously based on the conformational approach only, because both isomers of compound **2a** (*E* and *Z*) exist in a similar conformation with the cyclohexanone ring having an equatorial methyl group. Because of this steric repulsion between the equatorial methyl group at the chiral center of the CA molecule and the biphenyl fragment of the 5CB molecule can not differ appreciably. Nevertheless it was reported^{20,38} that owing to significantly different geometry of the isomers *Z*-**2a** and *E*-**2a** one can expect rather different electrostatic intermolecular interactions in corresponding LC systems. In the case of chiral additive *Z*-**2a** it is assumed³⁸ that intermolecular repulsion causing a clockwise rotation of the 5CB molecules relative to each other (right supramolecular helix) is provided by undesired interactions of the closely arranged benzene ring in the upper nematic molecule and carbonyl group, and the carbon atom of nitrile group bearing a partial positive charge with the likely charged carbon atom of the arylidene bond of CA.

* The character of repulsion between molecules in the model systems is illustrated in Refs 20 and 38.

The experimentally determined³⁸ relatively large absolute value of β for *Z*-**2a** is likely due to enhancement of intermolecular repulsion owing to better conditions for the 5CB and CA molecules to approach each other (strengthening of dispersion attraction) because of the lack of methyl group in α -position relative to the arylidene fragment. This is consistent with experimentally observed mesomorphic properties of alkyl-substituted compounds of the *E*-**2** type ($n = 6-11$) in contrast to non-mesomorphic isomenthone analogs *E*-**1**.^{15,20} An increase in steric repulsion between the CA *Z*-**2a**, and 5CB molecules and, hence, greater twisting in this case can also arise from the contribution of helical chirality due to a greater non-planarity of the enone fragment in *Z*-**2a** compared to *E*-**2a**. These effects are also most likely followed by suppression of mesomorphism of the *Z*-compounds (at least for *Z*-**2b**)⁷ unlike corresponding mesomorphic representatives of the *E*-**2** series.^{15,20}

Structural differences between the *E*- and *Z*-isomers of compounds **1** and **2** established in this work suggest that the axial or equatorial orientation of the methyl substituent in the cyclohexanone ring of chiral unsaturated ketones is not completely responsible for their twisting properties in LC systems. Specific features of polarization of the molecular fragments of chiral additives related to conformational differences and their electrostatic interactions with the molecules of the nematic environment also play an important role.

Experimental

Reaction mixtures were analyzed and the purity of the compounds synthesized was monitored by HPLC using a Milichrom-5 liquid chromatograph with a reversed-phase column Silasorb C-18 (2×6 mm) and a Bischoff HPLC system with a reversed-phase column Prontosil 120-5-C18 acE-EPS. Acetonitrile–water (70–100 vol.%) mixtures were used as eluents.

IR spectra were recorded with a Bruker IFS66 IR spectrometer in CCl₄ and UV spectra were measured with a Hitachi U3210 spectrophotometer in octane.

The twisting power was measured following a known procedure.²⁰

¹H NMR spectra were recorded with Varian Mercury-400 and Varian VXR-300 instruments (Me₄Si as internal reference). The proton multiplets in the second-order spectra were interpreted using the double resonance technique and confirmed by the computer simulation of spin systems using the NUTS 4.35c program. The multiplets of cyclohexanone ring protons were simulated using two spin subsystems, an eight-spin subsystem H_{eq}(2), H_{ax}(2), H_{eq}(4), H_{ax}(4), H(3), C(7)H₃ (in order to simulate the proton multiplets H_{ax}(2) and H(3)) and an eight-spin subsystem H_{eq}(2), H_{ax}(2), H(3), H_{eq}(4), H_{ax}(4), H_{eq}(5), H_{ax}(5), H(8) (in order to simulate the proton multiplets H_{eq}(2), H_{ax}(2), H_{eq}(4), H_{ax}(4), H_{eq}(5), H_{ax}(5), H(8)). The chemical shifts and spin-spin coupling constants were determined by an accuracy of 0.001 ppm and 0.1 Hz, respectively (according to calculations).

The starting structures of the compounds under study for optimization were composed using the HyperChem 5.01 program.⁴⁰ The structures of isomers and their conformers were found by full optimization of all geometric parameters by the semiempirical quantum chemical AM1⁴¹ and PM3⁴² methods implemented in the MOPAC 6.0 package.⁴³ Density functional quantum chemical calculations with the three-parameter functional B3LYP/cc-pVDZ were carried out using the GAUSSIAN 98 program.³⁵

The reagents used were commercially available (3*R*)-methylcyclohexanone (98%, [α]_D²⁴ +13.5) and 4-chlorobenzaldehyde (Sigma–Aldrich), 1,1'-bis(diphenylphosphino)ferrocene (DPPF), and K₃PO₄·(2–3)H₂O (Lancaster). Bis(triphenylphosphino)nickel(II) chloride NiCl₂(PPh₃)₂ was obtained following a known procedure.⁴⁴ Phenylboronic acid was synthesized by a known procedure.⁴⁵ Dioxane was purified from peroxides and dried following a conventional procedure.⁴⁶ Heptane (Merck) was used without additional purification.

(*E*)-2-(4-Chlorobenzylidene)-(5*R*)-methylcyclohexanone (4). A mixture of *p*-chlorobenzaldehyde (1.65 g, 12 mmol) and sodium hydroxide (0.8 g, 20 mmol) in water (50 mL) was degassed in a vacuum of a water jet pump and blown with argon (two or three cycles). Then, (3*R*)-methylcyclohexanone (2.7 g, 24 mmol) was added and the degassing procedure was repeated. The reaction mixture was boiled for 24 h with thorough stirring in argon atmosphere (HPLC monitoring), cooled, neutralized with acetic acid, and extracted with dichloromethane. The extracts were combined, washed with water until a neutral pH value, dried over CaCl₂, and then evaporated until dryness. The residue was recrystallized from a minimum amount of heptane to obtain 1.9 g (67%) of compound **4**. Further recrystallizations from heptane gave 1 g (36%) of a substance of analytically pure grade (>99%, HPLC data) as light yellow needle-shaped crystals, m.p. 63–64 °C (heptane) (*cf.* Ref. 14: m.p. 62–63 °C). ¹H NMR (CDCl₃, 300 MHz), δ : 7.61 (s, 1 H, C=CH); 7.04 (d, 2 H, H_o, ³*J* = 8.1 Hz); 6.85 (d, 2 H, H_m, ³*J* = 8.1 Hz); 3.00 (m, 1 H, H_{eq}(5)); 2.68 (m, 1 H, H_{ax}(5)); 2.62 (m, 1 H, H_{eq}(2)); 2.10 (m, 1 H, H_{ax}(2)); 2.06 (m, 1 H, H(3)); 1.92 (m, 1 H, H_{eq}(4)); 1.36 (m, 1 H, H_{ax}(4)); 1.05 (d, 3 H, Me, ³*J* = 6.1 Hz).

(*E*)-(5*R*)-Methyl-2-(4-phenylbenzylidene)cyclohexanone (*E*-2a**).** A mixture of bis(triphenylphosphino)nickel(II) chloride (84 mg, 0.128 mmol) and DPPF (78 mg, 0.141 mmol) was degassed in intense argon stream, anhydrous dioxane (3 mL) was added, and the mixture was degassed again. *n*-Butyllithium (2 *M* solution in hexane, 0.3 mL, 0.51 mmol) was injected into green NiCl₂(PPh₃)₂/DPPF suspension and the dark red mixture obtained was stirred for 10 min at ~20 °C; and then a mixture of chloride **4** (300 mg, 1.28 mmol), phenylboronic acid (172 mg, 1.41 mmol), and K₃PO₄·(2–3)H₂O (814 mg, 3.84 mmol) in 5 mL of dioxane degassed by bubbling argon was added. The reaction mixture was stirred for 8 h (HPLC monitoring; the change in the color of the reaction mixture from dark brown to light yellow, which was probably due to the decomposition of the catalyst to give anhydrous NiCl₂, served as visible indication of completion of the reaction), diluted with dichloromethane, and filtered through a layer of silica (Kieselgel, 0.035–0.070 mm, Acros Organics). The filtrate was evaporated to dryness. After evaporation, silica (S-120, 3 volumes) and a small volume of dichloromethane was added to the oily residue. The suspension obtained was evaporated *in vacuo* with stirring on a rotary evaporator at a bath temperature of at most 50 °C. The free-running

mass thus obtained was transferred to the column onto an S-120 silica layer and extracted with hot heptane. The extract was evaporated to dryness and the residue was recrystallized from acetonitrile until a maximum attainable purity (HPLC monitoring). The yield of ketone *E*-**2a** was 52%, purity >99% (HPLC data), m.p. 127–128 °C (from acetonitrile). IR, ν/cm^{-1} : 1600.8, 1625.0, 1680.6. UV, $\lambda_{\text{max}}/\text{nm}$ (ϵ): 243 (3515), 312 (25260). Twisting power (SCB), $\beta/\mu\text{m}^{-1}$ (mole fraction) $^{-1}$: -7.7 ± 0.5 .²⁰ ^1H NMR (CDCl_3 , 400 MHz), δ : 7.63 (d, 2 H, H_m , $^3J = 8.3$ Hz); 7.61 (d, 2 H, H_o , $^3J = 8.3$ Hz); 7.54 (s, 1 H, C=CH); 7.50 (d, 2 H, H_o , $^3J = 8.3$ Hz); 7.46 (d, 2 H, H_m , $^3J = 8.3$ Hz); 7.37 (t, 1 H, H_p , $^3J = 8.3$ Hz); 3.11 (m, 1 H, $H_{\text{eq}}(5)$); 2.71 (m, 1 H, $H_{\text{ax}}(5)$); 2.69 (m, 1 H, $H_{\text{eq}}(2)$); 2.12 (m, 1 H, $H_{\text{ax}}(2)$); 2.08 (m, 1 H, $H(3)$); 1.94 (m, 1 H, $H_{\text{eq}}(4)$); 1.39 (m, 1 H, $H_{\text{ax}}(4)$); 1.05 (d, 3 H, Me, $^3J = 6.2$ Hz).

(Z)-(5R)-Methyl-2-(4-phenylbenzylidene)cyclohexanone (Z-2a). A solution of *E*-**2a** (220 mg, 0.8 mmol) in 100 mL of heptane was exposed to unfiltered UV-radiation of a DRS-120 high pressure mercury lamp and stirred until a photostationary state (HPLC monitoring). Heptane was evaporated and the residue was crystallized from the minimum amount of methanol at -5 °C. The yield of ketone *Z*-**2a** was 14%, m.p. 70–71 °C (from methanol), purity 98% (HPLC data). IR, ν/cm^{-1} : 1626.2, 1654.9, 1695.2. UV, $\lambda_{\text{max}}/\text{nm}$ (ϵ): 258 (12980), 298 (25920). Twisting power (SCB), $\beta/\mu\text{m}^{-1}$ (mole fraction) $^{-1}$: 31.3 ± 1.5 .³⁸ ^1H NMR (CDCl_3 , 400 Hz), δ : 7.58 (d, 2 H, H_o , $^3J = 8.3$ Hz); 7.51 (d, 2 H, H_m , $^3J = 8.3$ Hz); 7.43 (d, 2 H, H_m , $^3J = 8.3$ Hz); 7.42 (d, 2 H, H_o , $^3J = 8.3$ Hz); 7.33 (t, 1 H, H_p , $^3J = 8.3$ Hz); 6.43 (s, 1 H, C=CH); 2.71 (m, 1 H, $H_{\text{eq}}(5)$); 2.63 (m, 1 H, $H_{\text{eq}}(2)$); 2.58 (m, 1 H, $H_{\text{ax}}(5)$); 2.27 (m, 1 H, $H_{\text{ax}}(2)$); 2.12 (m, 1 H, $H_{\text{ax}}(3)$); 2.01 (m, 1 H, $H_{\text{eq}}(4)$); 1.56 (m, 1 H, $H_{\text{ax}}(4)$); 1.08 (d, 3 H, Me, $^3J = 6.5$ Hz).

The authors express their gratitude to A. D. Roshal' for recording IR and UV spectra and to S. V. Iksanova for measuring the ^1H NMR spectrum of a semiproduct.

References

- G. S. Chilaya, *Fizicheskie svoystva i primeneniye zhidkikh kristallov s induktsirovannoi spiral'noi strukturoi* [Physical Properties and Applications of Liquid Crystals with Induced Helical Structure], Metsniereba, Tbilisi, 1985, 88 pp. (in Russian).
- G. M. Zharkova and A. S. Sonin, *Zhidkokristallicheskie kompozity* [Liquid-Crystalline Composites], Nauka, Novosibirsk, 1994, 214 pp. (in Russian).
- S. Superchi, M. I. Donnoli, G. Proni, G. P. Spada, and C. Rosini, *J. Org. Chem.*, 1999, **64**, 4762.
- L. A. Kutulya, in *Funktsional'nye materialy dlya nauki i tekhniki* [Functional Materials for Science and Technology], Ed. V. P. Seminozhenko, Institute for Single Crystals, Kharkov, 2001, 381 (in Russian).
- S. N. Yarmolenko, L. A. Kutulya, V. V. Vashchenko, and L. V. Chepeleva, *Liq. Cryst.*, 1994, **16**, 877.
- L. A. Kutulya, V. V. Vashchenko, A. O. Doroshenko, M. N. Pivnenko, L. V. Chepeleva, N. S. Pivnenko, and N. I. Shkolnikova, *Nonlinear Optics of Liquid and Photorefractive Crystals 2000*, SPIE Proc., 2001, **4418**, 89.
- A. I. Krivoshey, N. I. Shkolnikova, L. A. Kutulya, L. V. Chepeleva, and N. B. Novikova, *J. SID (USA)*, 2004, **12**, 173.
- A. I. Krivoshey, N. I. Shkolnikova, L. V. Chepeleva, L. A. Kutulya, and N. S. Pivnenko, *Funct. Mat.*, 2004, **11**, 76.
- J. Lub, W. Ten Hoeve, W. P. M. Nijssen, L. Diaz, and R. T. Wegh, *Liq. Cryst.*, 2002, **29**, 995.
- S. N. Yarmolenko, L. V. Chepeleva, L. A. Kutulya, V. V. Vashchenko, T. G. Drushlyak, and O. A. Ponomarev, *Zh. Obshch. Khim.*, 1995, **65**, 145 [*Russ. J. Gen. Chem.*, 1995, **65** (Engl. Transl.)].
- L. A. Kutulya, S. N. Yarmolenko, V. V. Vashchenko, L. V. Chepeleva, L. D. Patsenker, and O. A. Ponomarev, *Zh. Fiz. Khim.*, 1995, **69**, 88 [*Russ. J. Phys. Chem.*, 1995, **69** (Engl. Transl.)].
- N. S. Pivnenko, V. V. Vashchenko, L. A. Kutulya, A. O. Doroshenko, and L. V. Chepeleva, *Izv. Akad. Nauk, Ser. Khim.*, 2001, 1519 [*Russ. Chem. Bull., Int. Ed.*, 2001, **50**, 1596].
- N. S. Pivnenko, T. G. Drushlyak, L. A. Kutulya, V. V. Vashchenko, A. O. Doroshenko, and J. W. Goodby, *Magn. Reson. Chem.*, 2002, **40**, 566.
- N. S. Pivnenko, A. I. Krivoshey, and L. A. Kutulya, *Magn. Reson. Chem.*, 2003, **41**, 517.
- A. I. Krivoshey, L. A. Kutulya, V. V. Vashchenko, M. N. Pivnenko, N. S. Pivnenko, A. S. Tolochko, V. I. Kulishov, and N. I. Shkolnikova, *9th Int. Conf. «Nonlinear Optics of Liquid and Photorefractive Crystals» (Crimea, Ukraine, September–October, 2002)*, SPIE Proc., 2003, **5257**, 13.
- A. Beth, J. Pelletier, R. Russo, M. Soucy, and R. H. Burnell, *Can. J. Chem.*, 1975, **53**, 1504.
- F. Nerdel, B. Gnauck, and G. Kresze, *Justus Leibigs Ann. Chem.*, 1953, **580**, 35.
- S. Saito, S. Oh-tani, and N. Miyaura, *J. Org. Chem.*, 1997, **62**, 8024.
- E. V. Popova, L. A. Kutulya, M. N. Pivnenko, V. V. Vashchenko, and A. P. Fedoryako, *Proc. XI Int. Symp. "Advanced Display Technologies" (Crimea, Ukraine, September, 2002)*, P. 148.
- A. I. Krivoshei, Ph.D. (Chem.) Thesis, Scientific and Technological Corporation "Institute for Single Crystals", National Academy of Sciences of Ukraine, Kharkov, 2004, 162 pp. (in Russian).
- C. R. LeBlond, A. T. Andrews, Y. Sun, and J. R. Sowa, *Org. Lett.*, 2001, **3**, 1555.
- A. Hassner and T. C. Mead, *Tetrahedron*, 1964, **20**, 2201.
- P. Baas and H. Cerfontain, *Tetrahedron*, 1977, **33**, 1509.
- E. L. Eliel, N. L. Allinger, S. J. Angyal, and G. A. Morrison, *Conformational Analysis*, J. Wiley and Sons, New York—London—Sydney, 1965.
- W. B. Smith and C. Amezcua, *Magn. Reson. Chem.*, 1998, **3**, S3.
- W. B. Smith and C. Amezcua, *Magn. Reson. Chem.*, 1999, **37**, 110.
- R. J. Abraham and D. S. Ribeiro, *J. Chem. Soc., Perkin Trans. 2*, 2001, 302.
- D. S. Ribeiro, P. R. Olivato, and R. Rittner, *Magn. Reson. Chem.*, 2000, **38**, 627.
- S. V. Shishkina, T. G. Drushlyak, L. A. Kutulya, O. V. Shishkin, and J. W. Goodby, *Kristallografiya*, 2001, **46**, 834 [*Crystallogr. Repts*, 2001, **46** (Engl. Transl.)].
- C. A. G. Haasnoot, de F. A. A. M. Leeuw, and C. Altona, *Tetrahedron*, 1980, **36**, 2783.

31. R. H. Contreras and J. E. Peralta, *Progr. Nucl. Magn. Reson. Spectrosc.*, 2000, **37**, 321.
32. A. I. Krivoshey, L. A. Kutulya, N. I. Shkolnikova, and N. S. Pivnenko, *XVI Int. Conf. on Spectroscopy of Molecules and Crystals, SPIE Proc.*, Eds G. O. Puchkovska, T. A. Gavrilko, O. I. Lizengevich, and S. A. Kostyukevych, 2004, **5507**, 249.
33. G. A. Jeffrey, *J. Mol. Struct.*, 1999, **485–486**, 293.
34. G. R. Desiraju, *Chem. Commun.*, 2005, 2995.
35. M. J. Frisch, G. W. Trucks, H. B. Schlegel, G. E. Scuseria, M. A. Robb, J. R. Cheeseman, V. G. Zakrzewski, J. A. Montgomery, Jr., R. E. Stratmann, J. C. Burant, S. Dapprich, J. M. Millam, A. D. Daniels, K. N. Kudin, M. C. Strain, O. Farkas, J. Tomasi, V. Barone, M. Cossi, R. Cammi, B. Mennucci, C. Pomelli, C. Adamo, S. Clifford, J. Ochterski, G. A. Petersson, P. Y. Ayala, Q. Cui, K. Morokuma, P. Salvador, J. J. Dannenberg, D. K. Malick, A. D. Rabuck, K. Raghavachari, J. B. Foresman, J. Cioslowski, J. V. Ortiz, A. G. Baboul, B. B. Stefanov, G. Liu, A. Liashenko, P. Piskorz, I. Komaromi, R. Gomperts, R. L. S. Martin, D. J. Fox, T. Keith, M. A. Al-Laham, C. Y. Peng, A. Nanayakkara, M. Challacombe, P. M. W. Gill, B. Johnson, W. Chen, M. W. Wong, J. L. Andres, C. Gonzalez, M. Head-Gordon, E. S. Replogle, and J. A. Pople, *Gaussian 98, Revision A.11.1*, Gaussian, Inc., Pittsburgh (PA), 2001.
36. S. V. Shishkina, O. V. Shishkin, and J. Leszczynski, *Chem. Phys. Lett.*, 2002, **354**, 428.
37. R. F. W. Bader, *Atoms in Molecules. A Quantum Theory*, Clarendon Press, Oxford, 1990.
38. A. Krivoshey, N. Shkolnikova, N. Pivnenko, and L. Kutulya, *Mol. Cryst. Liq. Cryst.*, 2006, **449**, 21.
39. A. S. Tolochko, V. I. Kulishov, L. A. Kutulya, and V. P. Kuznetsov, V. V. Vashchenko, *Kristallografiya*, 2001, **46**, 254 [*Crystallogr. Repts*, 2001, **46**, 214 (Engl. Transl.)].
40. *HyperChem Reference Manual*, HyperCube Inc., 1996.
41. M. J. S. Dewar, E. G. Zoebisch, E. F. Healy, and J. J. P. Stewart, *J. Am. Chem. Soc.*, 1985, **107**, 3902.
42. J. J. P. Stewart, *J. Comput. Chem.*, 1989, **10**, 221.
43. J. J. P. Stewart, *QCPE Bull. (MOPAC 6.0)*, 1990, 455.
44. F. A. Cotton, O. D. Faut, and D. M. L. Goodgame, *J. Am. Chem. Soc.*, 1960, **83**, 344.
45. R. M. Washburn, *Adv. Chem.*, 1959, **23**, 102.
46. *Organikum. Organisch-chemisches Grundpraktikum*, VEB Deutscher Verlag der Wissenschaften, Berlin, 1976.

Received July 27, 2005;
in revised form May 17, 2006